Applied Catalysis B: Environment and Energy 344 (2024) 123636

Contents lists available at ScienceDirect

Applied Catalysis B: Environment and Energy

journal homepage: www.elsevier.com/locate/apcatb

Photothermal catalytic conversion of water and inert nitriles to amide activated by in-situ formed transition-metal-complex nanodots

Xiong-Feng Ma [a], Rui Xiao [a], Yingcong Wei [b], Shaohui Zhang [a], Xiaoyi Hu [a], Ling Zhang [a], Nanfang Qin [a], Lele Wang [b,*], Zhengxin Ding [a], Huaxiang Lin [a], Zizhong Zhang [a], Jinlin Long [a], Rusheng Yuan [a,*]

[a] State Key Laboratory of Photocatalysis on Energy and Environment, College of Chemistry, Fuzhou University, Fuzhou 350108, PR China
[b] School of Materials Science and Engineering, Jiangsu University, Zhenjiang, Jiangsu 212013, PR China

ARTICLE INFO

Keywords:
Amide synthesis
Transition-metal complexes nanodots
Photothermal catalysis
N-acyl sources
Photon–phonon coupling

ABSTRACT

Photothermal catalytic N-acetylation of aniline has been a promising strategy to synthesize amides, which combined the advantages of thermal catalysis and photocatalysis. Herein, we demonstrate a high-performance strategy to synthesize amides catalyzed by the in-situ formed first-row transition-metal (Fe, Co, Ni, Mn et al.) complexes nanodots (TMC NDs) under solar light excitation without using noble metals or strong acids. The dual-functional nitriles substrates acted as the ligands to coordinate with transition-metal salts affording photosensitive TMC NDs with high solar-to-thermal energy conversion efficiency. Intramolecular charge transitions reduced the energy barrier of nitriles activation by weakening C⩵N bond and triggered near-field temperature rise via the electron–phonon scattering non-radiative pathway. The reaction system exhibited good tolerance to different functional groups, affording a series of amide derivatives. Such a dynamic coordination reaction mode and the in-situ formed TMC NDs opens new avenues toward solar-heat conversion via photon–phonon coupling in the field of chemical synthesis.

1. Introduction

Using solar light to synthesize value-added, structurally complex organic compounds, especially via photothermal catalysis, is a promising approach for efficient solar-to-chemical energy conversion due to the synergistic effect of photocatalysis and thermal catalysis [1,2]. Amide group (-N-CO-) as the essential structural motif of the protein backbone can also be seen in the current drugs and diverse materials (Scheme 1a) [3–6]. The initial method to synthesize secondary amides in both industry and academia was the Beckmann rearrangement (BKR) of oxime which was first reported by Ernst Otto Beckmann in 1886 [7]. However, strong acids, toxic promoters, harsh reaction conditions and hazardous reagents are involved in BKR, thereby limiting its general applicability [8]. Alternatively, amides have also been synthesized by the carbonylation of amines with CO as the carbonyl source (Scheme 1b) [9]. These gas–liquid–solid multiphase reaction models have exhibited a high interface energy barrier, and the high bond-dissociation energy of CO (1072 kJ·mol^{-1}) restricted the kinetics of amide synthesis, thereby leading to a low catalytic efficiency [10,11]. Therefore, designing and implementing an applicable synthetic approach involving milder reaction conditions and the use of widely available CO-gas-free acetyl sources enabled by a solar-driven catalytic process remain challenging and hence attracts considerable attention.

Recently, a series of liquid- or solid-phase starting materials such as acid chlorides, anhydrides or carboxylic acids instead of CO were employed as acetyl sources for amide synthesis in the presence of an acid or a base promoter (Scheme 1b) [8,12]. However, these substrates exhibited inherent disadvantages such as limited functional group compatibility, poor atom economy, and increased the operator's exposure to toxic chemicals, consequently, the scope of these reactions was limited [13–16]. Moreover, most of the oximes used as starting materials are solids with high melting points, which make them almost insoluble in most organic solvents [17]. A study was reported on the catalytic oxidation of alcohols employing water as the oxygen atom source by D. Milstein and co-workers, thus, a potentially attractive synthetic approach for amides is to consider water as the oxygen atom donor for the carbonyl group [18]. J. You and coworkers reported the transfer of nitrogen to various aldehydes via the cleavage of the C⩵N bond, thereby

* Corresponding authors.
E-mail addresses: 1000005351@ujs.edu.cn (L. Wang), yuanrs@fzu.edu.cn (R. Yuan).

https://doi.org/10.1016/j.apcatb.2023.123636
Received 22 August 2023; Received in revised form 14 November 2023; Accepted 15 December 2023
Available online 19 December 2023

eliciting possibilities for the application of nitriles as the source of N for generating amides [19]. However, the use of chemically inert nitrile and molecular water as N-acyl sources for the photothermal catalytic synthesis of amides has been rarely reported so far.

In addition to the optimization of N-acyl sources, the development of high efficient photothermal catalysts is important for amide synthesis. Generally, noble-metal-based catalysts, such as Au/TiO_2 [20], $[Ru(benzene)Cl_2]_2$ [21] or N-heterocyclic carbine (NHC)–Ru complex [22,23], are used in the photocatalytic or thermal catalytic amide synthesis. Prohibiting from the rich redox states, abundant and nontoxic first-row transition metal (TM)-based materials (derived from Fe, Co, Ni, Cu, Mn et al.) are expected to replace noble-metal-based catalysts in the organic catalytic transformations [24]. Recently, a work on Nature reported by Gregory C. Fu and co-workers showed the possibility of amide formation efficiently driven by copper-based complex under light irradiation which indicated the potential for the application of transition metal-based photocatalysts in amides synthesis [25]. Further, various ligands with complex structures were designed to tune the redox and light absorption ability of transition metal-based complexes (TMC) [26–28], few of them exhibited higher activity than those of the well-established noble metal catalysts, and nearly none of them exhibited photothermal effect except the reported photothermal materials including plasmonic metals [29], stoichiometric/nonstoichiometric semiconductors [30–32], and the MXenes [33] (Scheme 1c). Interestingly, Yuan's group reported that TMC NDs (2–8 nm) generated by the self-assembly of TMC molecules can exhibit a high photocatalytic efficiency for carbonylation via intramolecular charge transfer [34]. Considering that traditional nanostructured photothermal catalysts can convert solar energy into heat via different mechanisms such as plasmonic localized heating, nonradiative relaxation in semiconductors, and thermal vibration of molecules, the as-formed TMC NDs are speculated to demonstrate the potential to serve as the photothermal catalysts [35]. Taking inspiration from these works, one can predict that once the bifunctional ligand (nitrile) is used as the acetyl source, the photosensitive iron-based complex NDs formed in situ will exhibit excellent photothermal performance for amide synthesis.

Herein, we demonstrate an effective strategy to achieve solar-driven amides synthesis with nitrile and H_2O as the N-acyl group sources catalyzed by the in-situ formed TMC NDs (derived from Fe, Co, Cu, etc.) (Scheme 1d). The formed metal–acetonitrile complex molecules could spontaneously aggregate into NDs with an average dimeter in the range of 1.5–2.4 nm. Prohibiting from the nonradiative energy dissipation pathway, the electron–phonon scattering in the TMC NDs afforded a high solar-to-thermal energy conversion efficiency, thus remarkably increased the temperature of the reaction mixture (the highest photothermal conversion efficiency (PCE) can reach to 45.8%). Under solar

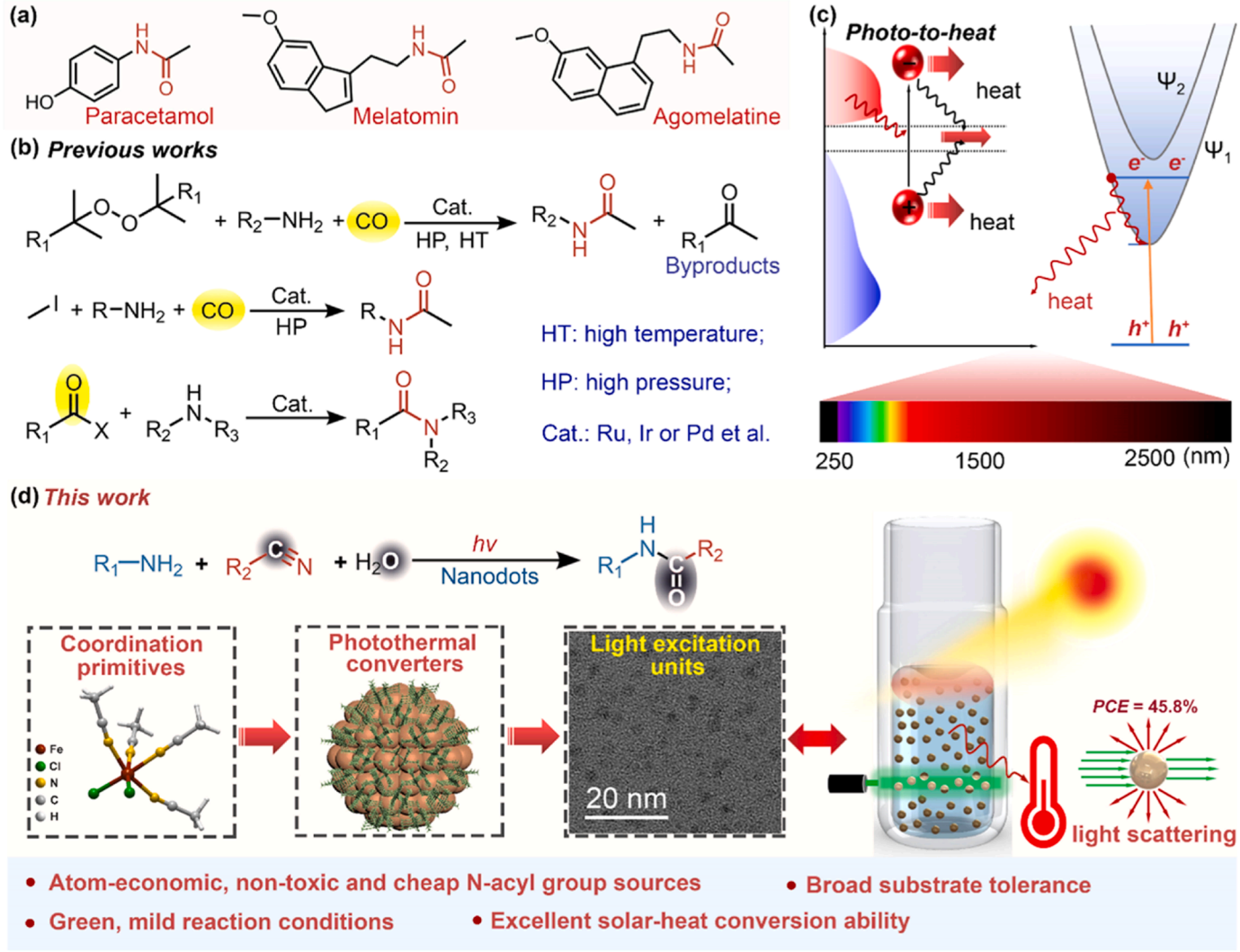

Scheme 1. (a) Typical drugs containing N-acetyl moiety; (b) Schematic illustration of the electronic structure and the solar-heat energy conversion mechanism of TMC NDs; (c) Previous reports on amide synthesis; (d) New strategies for the amide synthesis and the formation of TMC NDs through molecular aggregation.

light irradiation, the NDs could drive the acetylation of amine, affording amides with high yields (493–926 μmol). Isotopic labeling studies were conducted to investigate the N-acyl sources for amides. High Resolution Mass Spectra (HR-MS) were obtained to analyze the reaction intermediates during the reaction. Based on density functional theory (DFT) calculations and experimental results, a plausible reaction mechanism is proposed. Such a solar light-driven acetylation strategy could serve as an effective, green and economical method for amides synthesis.

2. Experimental section

2.1. Materials and reagents

All metal salts including $FeCl_3{\cdot}6\ H_2O$, $Fe(NO_3)_3{\cdot}9\ H_2O$, $CuCl_2{\cdot}2\ H_2O$, $NbCl_5$, $TaCl_5$, $CrCl_3{\cdot}6\ H_2O$, $MnCl_2{\cdot}4\ H_2O$, $CoCl_2{\cdot}6\ H_2O$, $NiCl_2{\cdot}6\ H_2O$, $FeBr_3$, $CdCl_2{\cdot}2.5\ H_2O$, $ZnCl_2$, $FeCl_3$, CuCl were obtained from Sigma-Aldrich, Alfa Aesar and Aladdin (analytical grade) and are in storage in the N_2-filled glovebox at 25 °C. The amines substrates, nitrile, Nessler's reagent and certain solvents obtained from commercial suppliers (Aladdin, Innochem) were dried by the vacuum rotary evaporator and stored in the N_2-filled glovebox. Other reagents were purchased commercially (Sigma-Aldrich) and used without other processing. All glassware used in the reactions was completely dried. The circulating cooling device was used to provide a low and constant temperature of the surrounding environment when certain control reaction was performed. The oil bath was used to provide high temperature during the thermal-driven reactions. Other experimental details for reaction conditions and the characterization details can be seen in the Supporting Information.

2.2. Experimental procedures for acetylation reaction of aniline

Generally, 0.2 mmol of $FeCl_3{\cdot}6\ H_2O$, 0.5 mL CH_3CN and 2 mL aniline were added to a 25 mL Schlenk tube charged with a magnetic stirrer. The resulting mixture was stirred upon UV–vis–NIR light (300–1050 nm) irradiation with an illuminated area of about 2 cm^2 corresponding to the cross section of the column tube. After 24 h reaction, the resulting reaction mixture was centrifugalized and the as-obtained supernatant liquid was identified by GC, GC-MS and NMR, respectively. The reactions and separation procedures under thermal conditions were similar to those described in the photoreactions except that light was replaced by heat using oil bath.

2.3. Chromogenic reactions to investigate the final chemical state of N in CH_3CN

Typically, photocatalytic acetylation reaction was conducted under standard reaction conditions. After 24 h of reaction, a certain volume of the reaction solution was collected, filtered and extracted by 2 mL of H_2O. After layered, the water phase was collected and analyzed by Nessler's reagent with the concentration of 0.09 $mol{\cdot}L^{-1}$ K_2HgI_4 and 2.5 $mol{\cdot}L^{-1}$ KOH. Briefly, 5 mL of the above reactive solution was added into a 20 mL colorimetric tube, followed by successive addition of 0.1 mL of Nessler's reagent and ultrapure water. The color change of the mixture before and after the addition of Nessler's reagent was recorded by taking photos. For comparison, the NH_4Cl solution with a concentration of 1 $mol{\cdot}L^{-1}$ was also analyzed by the Nessler's reagent. Generally, the color change from colorless to brown indicated that the formed NH_4^+ reacted with the HgI_4^{2-} and OH^-, as provided in the following equation.

$$2HgI_4^{2-}+NH_4^++4OH^-=Hg_2NI\ H_2O+7I^-+3\ H_2O$$

3. Results and discussion

A series of TM salts (such as $FeCl_3{\cdot}6\ H_2O$, $Fe(NO_3)_3{\cdot}9\ H_2O$, $CuCl_2{\cdot}2\ H_2O$, $NbCl_5$, $CrCl_3{\cdot}6\ H_2O$ and $CoCl_2{\cdot}6\ H_2O$) coordinated with acetonitrile, affording the corresponding NDs with the diameter ranging from 1.5 to 2.4 nm (Fig. 1a-f), which was consistent with that reported in our previous work [34]. TEM images of $FeCl_3$-CH_3CN solution with different $FeCl_3{\cdot}6\ H_2O$ concentrations showed that the size of TMC NDs was up to 2.2 nm (1.5 $\mu mol{\cdot}mL^{-1}$), and the NDs aggregated into nanorods when the $FeCl_3$ concentration increased to 15 and 30 $\mu mol{\cdot}mL^{-1}$ (Fig. 1a and Fig. S1). Elemental mapping as well as the X-ray photoelectron spectroscopy (XPS) survey spectrum of the NDs confirmed that the NDs and TMC molecules bear the same elemental composition (Fe, Cl, N, C), suggesting that these NDs composed of TMC molecules (Fig. 1g and h, and Fig. S2). Compared with the simulated XRD patterns of $FeCl_3$-CH_3CN complexes, the obtained NDs showed the same diffraction peaks with $FeCl_3$-CH_3CN complexes, further conforming the chemical composition of the NDs in the acetonitrile solutions (Fig. 1i). Relevant absorption band originated from the *d*(Fe)-*p*(N) transition band, wworks reported by our group revealed that these TMC molecules can aggregate via the Fe–Cl–Fe bridge bonding to form NDs aggregates under an exothermic reaction and spontaneous processes [34]. As expected, the solution containing TMC NDs exhibited a wide spectral absorption range (200–700 nm). According to time-dependent DFT calculations, thehich indicates a promising strategy for full-spectrum photons conversion in chemical transformations (Fig. 1j and Fig. S3).

The redox performance of various TMC NDs were tested using the acetylation of aniline under solar light irradiation. To our delight, the acetylation of aniline with acetonitrile and water proceeded smoothly using different TMC NDs under UV-Vis-NIR light irradiation (Fig. 2a). The desired acetylized product **3a** (N-phenyl-acetamide) with a yield of 525 μmol was obtained in the presence of $FeCl_3$, the amount of which was greater than those produced using other TM salts. No product was obtained in the absence of TM salts, nitrile or H_2O, indicating that the formed TMC NDs may be the active sites, and nitrile as well as trace of H_2O may serve as the N-acyl sources during the reaction. When air was replaced by N_2, no notable loss in the reactivity was observed,

suggesting that oxygen atom in **3a** possibly originated from H_2O rather than molecular oxygen (Fig. 2a and S4). To improve the yield of this reaction, contributing factors—such as incident light intensity, reaction time, solvents, light wavelength, additive and reaction temperature—that could affect the yield of **3a** were further optimized (Fig. 2 and Fig. S5-S9, Table S1). When solvents such as acetone, ethanol, DMF, DMSO, trichloromethane and cyclohexane were added to the reaction mixture respectively, a considerably lower efficiency or no efficiency was observed for the acetylation of aniline (Fig. S7). In addition, the reactions were conducted under incident lights excitation of different wavelengths (Table S2). Both 254, 365 nm and visible light (420–780 nm) initiated the reaction, affording a small amount of **3a**. Even under NIR-light excitation, the reaction can also take place and afford **3a** with an amount of 231 μmol (Fig. S8). Interestingly, a small amount of acid dramatically enhanced the reactivity, while a base hardly affected the reaction (Fig. S9). Considering that the addition of acid always leads to equipment corrosion, which limits industrial application of this method, acid or additives were not involved in the subsequent reactions.

Generally, heat is beneficial for photocatalysis via providing high kinetic energy to the photogenerated charges, thus improving the charge carrier mobility and catalytic performance [36–39]. Therefore, control experiments were conducted to explore the role of temperature in the acetylation reaction (Fig. 2b). Under dark conditions, the reaction didn't occur below 60 °C (Table S2). When the reaction temperature exceeds 60 °C, the reaction can take place smoothly and the highest amount of **3a** (336 μmol) was obtained at 100 °C. However, at a reaction temperature of > 100 °C, the yield of **3a** decreased possibly because a reaction temperature greater than the boiling point of aniline led to the

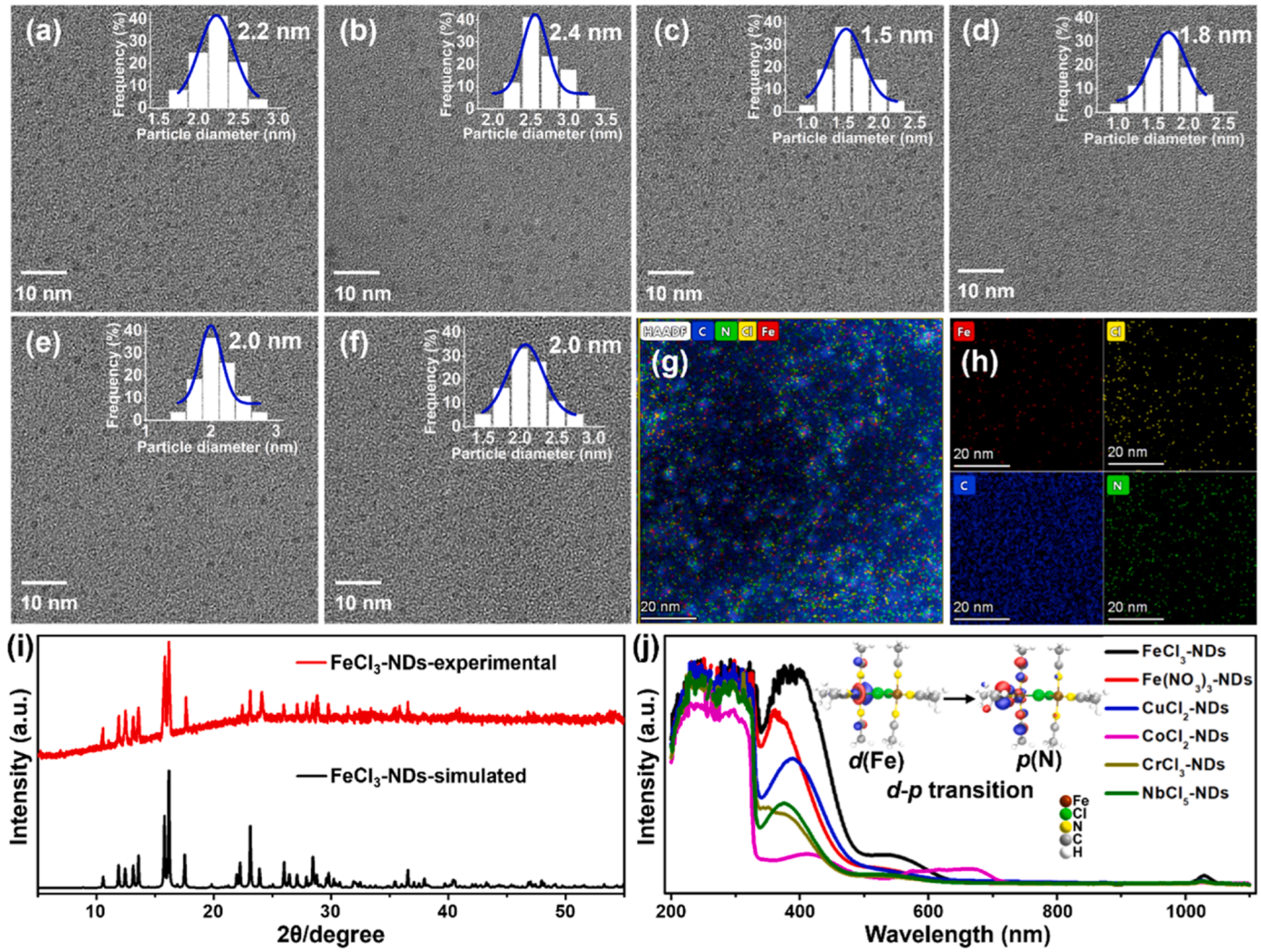

Fig. 1. TEM images of CH_3CN solutions containing $FeCl_3·6\ H_2O$ (a), $Fe(NO_3)_3·9\ H_2O$ (b), $CuCl_2·2\ H_2O$ (c), $NbCl_5$ (d), $CrCl_3·6\ H_2O$ (e) and $CoCl_2·6\ H_2O$ (f); (g, h) Elemental mapping results of the $FeCl_3$-CH_3CN NDs; (i) Experimental and simulated XRD pattern of the $FeCl_3$-CH_3CN complex; (j) The corresponding absorption spectra of CH_3CN solutions containing different kinds of metal salts, inset is the molecular model of $FeCl_3$-CH_3CN complex dimer.

volatilization of the substrate, resulting in lower production. These results indicated that heating also contributed to substrate activation. Inspired by the above results, a series of experiments were designed to further identify the role of incident photons and heating on the reaction. The comparation of different reaction conditions for solar light irradiation and heating revealed that 525 μmol **3a** was obtained under the former condition, which is 1.8 times higher than that obtained under the later condition (Fig. 2b). When the reaction temperature was controlled at room temperature (25 °C) by water cooling device under solar light, no **3a** can be observed after 24 h reaction (Table S2). This result suggested that incident photon electrons play a key role in driving the reaction. It is worth noting that, during the reaction, the temperature of the reaction mixture under solar light irradiation can reach to 101 °C, and the reaction temperature under heating conditions was also maintained at 101 °C. Based on these results, one can safely conclude that the TMC NDs could convert photons to heat via photon-phonon coupling, and the acetylation of amine undergo the photothermal synthesis process. Generally, in the process of photon-phonon coupling, the incident photons would interact with the crystal lattice of the complex nanodots, increasing the frequency and amplitude of lattice vibrations. During the transmission of the lattice vibration, the energy of the photons would transfer to the surrounding lattice or other phonons, thus facilitating the energy transfer and relaxation. Followed by the energy relaxation process which as a form of energy conversion and dissipation in the photon-phonon coupling results in temperature increase in the surrounding medium [40–42]. Such an explanation tells how the TMC NDs can convert incident photons into heat increasing the temperature of the systems.

Moreover, the absorbed light not only generated charges that participated in the activation of substrates but also induced electron–phonon scattering, thus trigger near-field temperature rise in the reaction system. By conducting the reaction in a scaled-up model, gram scale target **3a** (17.8 g) was obtained with the highest turnover number (TON) of up to 655 (Fig. 2c). Interestingly, under solar light-driven semicontinuous-flow reaction conditions, **3a** was produced at a rate of 549.4 $\mu mol \cdot h^{-1}$ (Fig. 2d). All of the results revealed that the TMC NDs may possess a photothermal conversion ability, which resulted in amide synthesis with high efficiency.

Inspired by the above results, the photothermal behavior of the TMC NDs in the mixture of CH_3CN and aniline (1:3 vol ratio) was evaluated. Under simulated solar light irradiation, the temperature of the solution containing different TMC NDs (viz. $FeCl_3$–CH_3CN NDs, $Fe(NO_3)_3$–CH_3CN NDs, $CoCl_2$–CH_3CN NDs, $CuCl_2$–CH_3CN NDs, and $NbCl_5$–CH_3CN NDs) increased more significantly than that of the bare solution within 10 min (Figs. 2e and 2f, Fig. S10). Especially for the $FeCl_3$–CH_3CN NDs, the temperature rose from 25 °C to 98 °C after solar

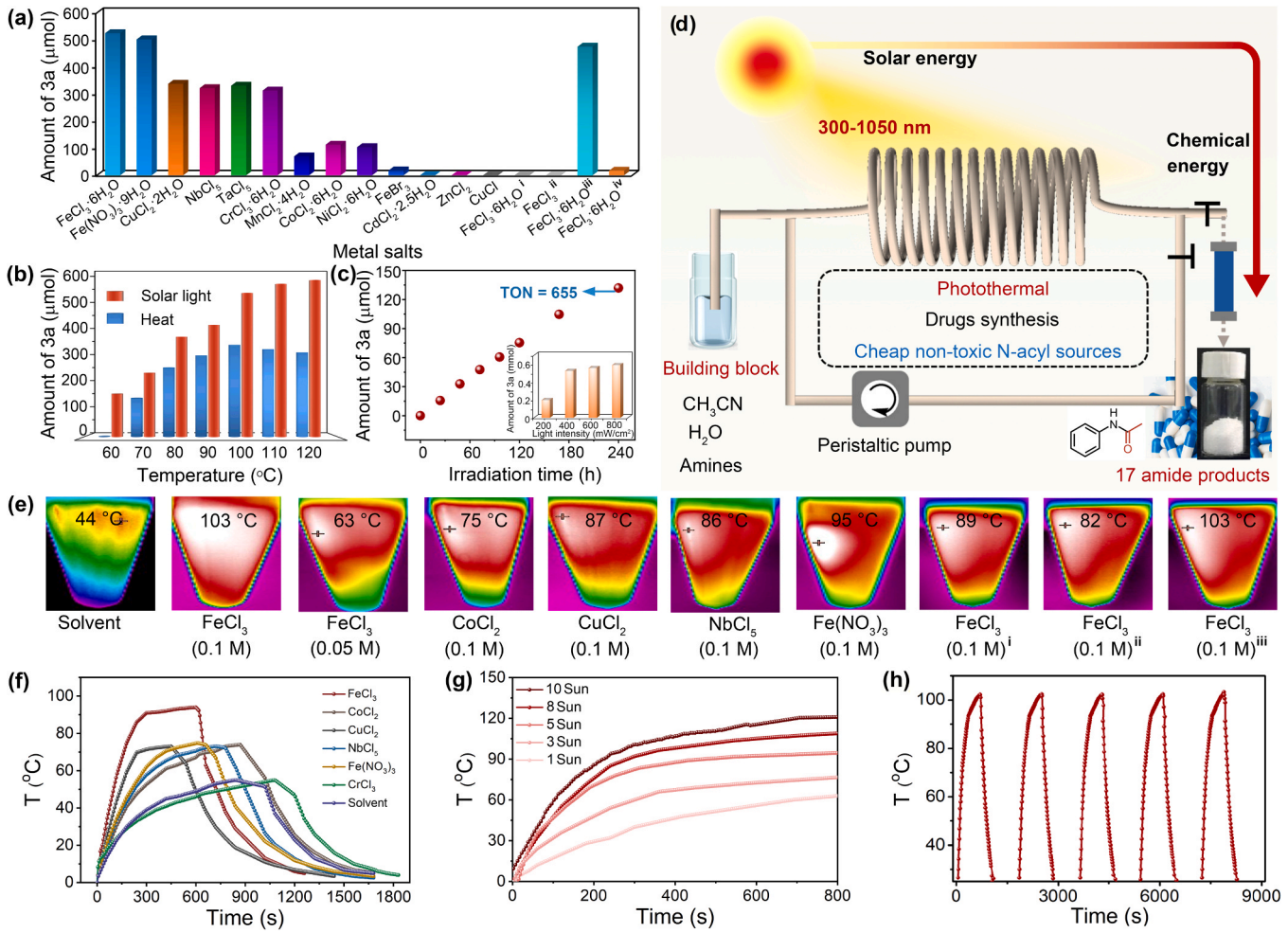

Fig. 2. (a) The acetylation reaction performance with different catalysts: [i] Without CH_3CN, [ii] $FeCl_3$ instead of $FeCl_3{\cdot}6\,H_2O$, [iii] N_2 atmosphere, [iv] 254 nm light instead of 420–780 nm light; (b) Comparation of solar light irradiation and heating on the production of 3a; (c) Scaled up acetylation reactions: 10 mL CH_3CN, 30 mL aniline, 4 mmol $FeCl_3{\cdot}6\,H_2O$, 300–1050 nm, and impact of light intensity of incident light on amount of 3a (inset); (d) Diagram for solar light driven acetylation reaction in semi-continuous flow mode; (e) Photothermal imaging of different solutions at 10 min under light irradiation (300–1050 nm), [i] 320–650 nm light irradiation, [ii] 650–1050 nm light irradiation, [iii] 300–1050 nm light irradiation; (f) Temperature change curves of different samples; (g) Temperature change curves of $FeCl_3$-CH_3CN NDs under different light intensities; (h) Photothermal stability of $FeCl_3$-CH_3CN NDs after five runs light irradiation.

light or 450 nm single-wavelength irradiation for 7 min, which shows higher solar-heat conversion efficiency than that of $Fe(NO_3)_3$-CH_3CN NDs, $CuCl_2$-CH_3CN NDs, $CoCl_2$-CH_3CN NDs and $NbCl_5$-CH_3CN NDs, respectively. With increasing solar illumination intensities from 1 sun (300–1050 nm, 100 $mW{\cdot}cm^{-1}$) to 10 sun, the temperature of the sample considerably increased, and the highest PCE (η) of $FeCl_3$-CH_3CN NDs was up to 45.8% (the calculation detail can be seen in the Suppoting Information), validating the significant Vis-NIR light-to-thermal energy conversion efficiency (Fig. 2g). The trend of temperature increase at different wavelengths was consistent with that of the absorption spectrum (Fig. 2e and Fig. S11). This phenomenon indicated that the characteristics of photothermal effect were positively correlated with the number of incident photons. With increasing TMC NDs concentration, the temperature increased (Fig. 2e). All these evidences confirmed that TMC NDs materials can not only utilize extended light absorption to generate charge carriers but also convert the absorbed photon energy into heat to accelerate the photocatalytic reaction, which is in accordance with the performance of the $FeCl_3$–based solution for the acetylation of aniline. In addition, the light-induced temperature rise process and the cooling process were recorded to investigate the photothermal stability of the TMC NDs (Fig. 2h). No obvious decay in temperature increase was observed after five cycles of light irradiation, suggesting the good photostability of the TMC NDs in the mixed solution. The excellent temperature increases originating from the high-efficiency solar-to-thermal energy conversion and the exothermic process of the reaction (Fig. S12 and S13, Table S3 and S4) facilitated the separation of photogenerated charges and thus showed immense potential in photo-induced synthetic reactions.

Under the optimized reaction conditions, the substrate scope and versatility of this methodology were assessed. All the primary amines (2-phenylethylamine, 3-penyl-propylamine and 1-heptylamine) and tertiary amines (benzylamine, piperidine, heptamethyleneimine, morpholine and thiomorpholine) could be activated and afforded amides in moderate-to-good yields (Table 1, **3a-3q**). Thiomorpholine afforded the product with the highest yield of up to 926 μmol (**3 h**). When acetonitrile was replaced by benzonitrile, a slightly lower yield of benzanilide was obtained (**3 l**). Using phenylacetonitrile as the acyl source, 509 μmol of N-phenylbenzeneacetamide was obtained (**3 m**). Surprisingly, paracetamol (acetaminophen) was also synthesized with a high yield (472 μmol), which as an effective analgesic was widely encountered in pharmaceuticals, especially when administered i.v. and in a broad range of clinical conditions (**3o**). In addition, 431 μmol of the melatonin (N-acetyl-3-(2-aminoethyl)– 5-methoxyindole) and 137 μmol of agomelatine (beta-methyl-6-chloromelatonin) were also obtained under the same reaction conditions, exhibiting biological activity as a neurohormone, a chronobiotic and an antioxidant (**3p** and **3q**). All

Table 1
Acetylation reaction of amines and nitrile.

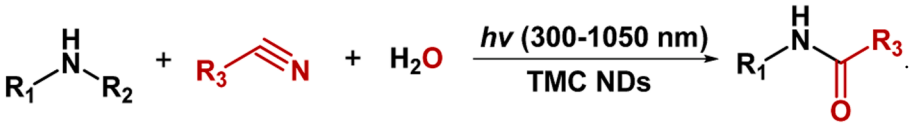

Entry	Amines	Product	Amount of amide (μmol)	Entry	Amines	Product	Amount of amide (μmol)
1	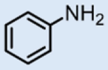	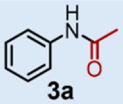 3a	525	10	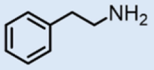	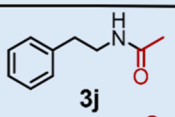 3j	607
2	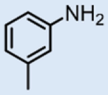	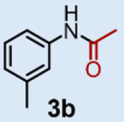 3b	547	11	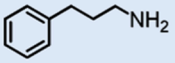	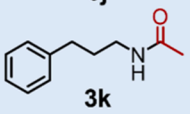 3k	621
3	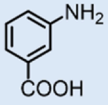	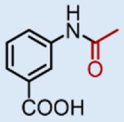 3c	563	12 [i]	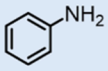	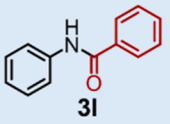 3l	493
4	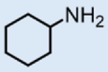	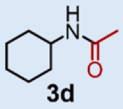 3d	582	13 [ii]	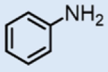	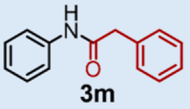 3m	509
5	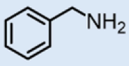	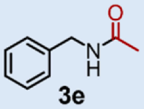 3e	556	14	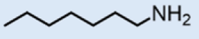	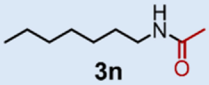 3n	643
6		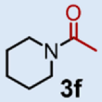 3f	726	15	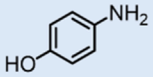	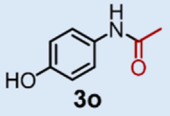 3o	472
7		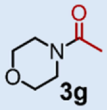 3g	865	16	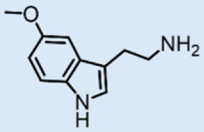	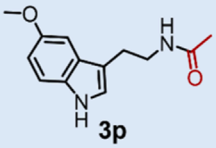 3p	431
8		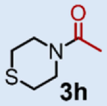 3h	926	17 [iii]	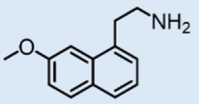	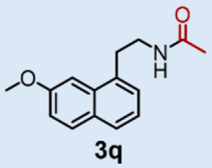 3q	137
9		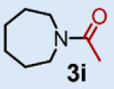 3i	597				

these results indicated that the TMC NDs–catalyzed reaction system exhibited a wide substrate scope, and the N elements in the final products were derived from the amine substrates rather than from nitrile.

To investigate the N-acetyl sources in the N-phenyl-acetamide product, isotope-labeling studies were performed using CD_3CN instead of CH_3CN as the substrate. As shown in Fig. 3a, when the reaction was conducted using CD_3CN, labeled N-phenyl-acetamide (ph-N-CO-CD_3, *MW*=138.1) was detected after 24 h′ irradiation while unlabeled **3a** (*MW*=135.1) was detected under the same reaction conditions using CH_3CN. A control experiment was also performed by irradiating the mixture of N-phenyl-acetamide and CD_3CN. No labeled product (ph-N-CO-CD_3) was obtained, indicating that the CD_3 group in CD_3CN can't be transferred to the **3a** product in the reaction system. The above experimental evidences implied that CH_3CN serving as the N-acyl source was incorporated into the final product during the photocatalytic acetylation of aniline.

General reaction conditions: 1.5 mL amine, 0.5 mL nitrile, 0.2 mmol $FeCl_3{\cdot}6\ H_2O$, air atmosphere, 300–1050 nm light irradiated for 24 h (400 mW·cm^{-2}), isolated amount of amides; [i] 1.5 mL aniline, 0.5 mL benzonitrile; [ii] 1.5 mL aniline, 0.5 mL phenylacetonitrile; [iii] 0.25 mL CH_3CN, 0.2 mmol amine, 1 mL DMF.

In addition, control experiments were conducted to further confirm the O and N source of acyl group. As shown in Fig. 3b, when the reaction was conducted under anhydrous conditions, no final product was obtained and only N,N′-diphenylacetamidine was detected in the LC-MS spectrum. However, trace of water could afford **3a** with a satisfactory yield, and the production of **3a** increased with increasing of H_2O concentration. These results indicated that the O element in the amide products originated from the introduced H_2O in the regents or salts. This result could also be confirmed by the isotope labeling experiments using H_2O^{18} as the substrate, in which the ph-N-CO^{18}-CH_3 was obtained instead of ph-N-CO-CH_3 (Fig. 3c). In addition, when N^{15} labeled aniline was used as the starting material, N^{15} labeled N^{15}-phenyl-acetamide (ph-N^{15}-CO-CH_3, *MW.* = 136.1) was observed in the GC-MS spectrum after reaction, indicating the N element derived from the amine substrate (Fig. S14). Such a synthetic method with H_2O and CH_3CN served

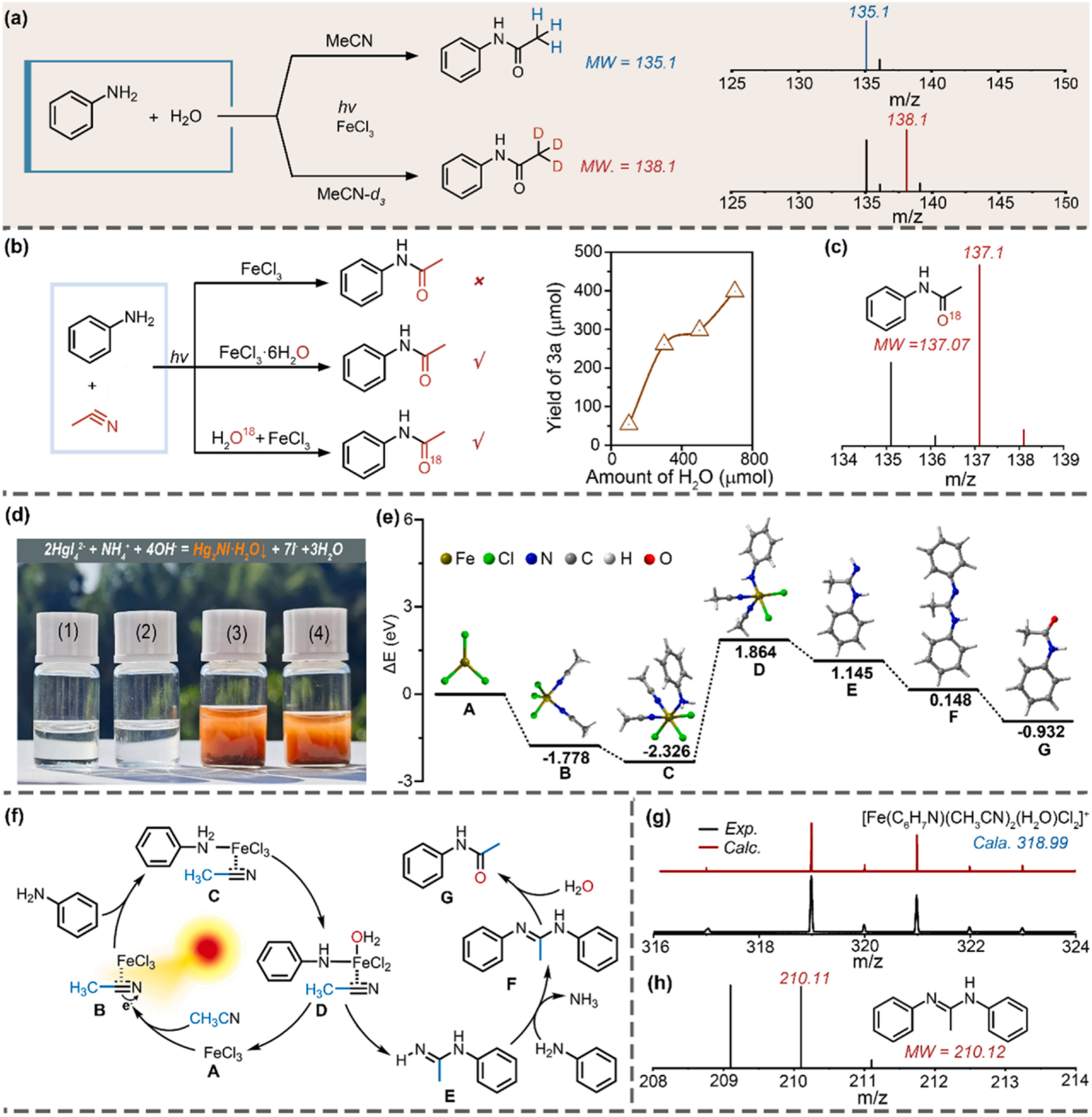

Fig. 3. (a) GC-MS spectra of the products when the reaction conducted under an isotopic tracer technique using CH_3CN and CD_3CN; (b) Control experiments of the O source of acyl group; (c) Isotope-labeling experiments for the O source in amide; (d) Identification of NH_4^+ ions after reaction; (e, f) Plausible mechanism and reaction pathway for the photothermal conversion of amine and nitrile to amides; (g, h) HR-MS spectra of key intermediates during the reaction.

as the source of acetyl group in the final products would attract attention in terms of atomic economy [27,43].

The final chemical form of N elements in acetonitrile was also investigated. Initially, the reaction was conducted under different atmospheres such as air and NH_3, the reaction was inhibited only under NH_3 and the reaction was not affected by other gas atmospheres (Fig. S3). This result may be attributed to the possible increase in the pH of the reaction mixture by the introduction of ammonia, which prevented acetylation. To further confirm this speculation, Na_2CO_3 was added into the reaction mixture to provide a basic environment and acetylation reaction proceeded smoothly under O_2, which ruled out this possibility (Fig. S15). Generally, when one of the final products was introduced into the reaction mixture, the reversible reactions tended to occur in the opposite direction which led to reduced or no final products. Based on the present results, we reasoned that NH_3 or NH_4^+ were generated during the reaction. The chromogenic reaction was conducted via adding the Nessler's reagent (K_2HgI_4) into the extracted reaction mixture (Fig. 3d) [44]. The color change from colorless to orange-yellow, attributed to the formation of colored complex (NH_2-Hg_2I_3), confirmed that the final chemical form of N in acetone was

NH_4^+ rather than N_2 or other compounds.

Based on these experimental results, the plausible reaction pathway for the photothermal conversion of amine and nitrile to amides was calculated. As shown in Fig. 3e, the intermediates and transition states were also predicted. Initially, when $FeCl_3$ (A) was dissolved into acetonitrile, the $FeCl_3$–acetonitrile complex NDs (B) were formed with the formation energy (ΔE) value of 1.778 eV, and the negative value suggested an exothermic reaction process (Fig. 3f). Then, the coordination of A with amine take place, generating $[Fe(C_6H_7N)(CH_3CN)_2Cl_3]$ intermediate (C). Upon light irradiation, protonation and coordination of the intermediate with molecular H_2O occurred, affording the $[Fe(C_6H_6N)(CH_3CN)_2Cl_2(H_2O)]$ (D) intermediate and HCl, which was confirmed by the LC-MS spectrum of the reaction mixture (Fig. 3g). Followed by the formation of N-phenylacetimidamide intermediate (E) and $FeCl_3$. After the substitution reaction of aniline, the N,N′-diphenylacetamidine was formed as the key intermediate (F)and ammonia was released, as confirmed by the GC-MS spectra of the reaction mixture (Fig. 3h). Finally, the subsequent hydrolysis took place, leading to the formation of N-phenyl-acetamide (G). Simultaneously, the obtained $FeCl_3$ coordinated with acetonitrile in a new reaction cycle. During the catalytic process, the Fe salt played an important role in activating acetonitrile via the coordination process, and the formed complex NDs exhibited a high solar-to-thermal energy conversion efficiency, which boosted the electron transfer and proton transfer process and benefited amide formation.

4. Conclusion

In conclusion, we successfully accomplished solar-light driven N-acylation of amine using nitriles and H_2O to afford various amides in good to excellent yields under photothermal reaction conditions. The TMC NDs formed via the self-assembly of TMC molecules as a new photothermal material exhibited high solar-to-thermal energy conversion efficiency, which accelerated the charge and proton transfer during the reaction. The nitriles and molecular H_2O served as N-acyl sources, avoiding the reliance on toxic starting materials. The mechanism for amide synthesis had been investigated, and the experimental results revealed that the N,N′-diphenylacetamidine intermediate formed during the photothermal process was the key intermediate that led to the formation of amides. Such a dynamic coordination reaction mode highlights the possibility of controlling reactions at the single-molecule level and opens new avenues toward solar-to-thermal energy conversion for the application of photon-phonon coupling in the field of chemical synthesis.

Author contributions

R.Y. conceived and initiated the research. L.W. and X.M. performed the experiments and wrote the manuscript. R.X., Y.W., S.Z., L.Z., N.Q., H.L. and Z.D. analyzed the data. X.H. performed the DFT calculations. Z. Z. and J.L. discussed and revised the manuscript.

CRediT authorship contribution statement

Rusheng Yuan: Conceptualization, Formal analysis, Funding acquisition, Writing – review & editing. **Lele Wang**: Data curation, Formal analysis, Writing – original draft. **Xiong-Feng Ma**: Data curation, Formal analysis, Writing – original draft. **Rui Xiao**: Data curation, Formal analysis. **Yingcong Wei**: Data curation, Formal analysis. **Shaohui Zhang**: Formal analysis. **Xiaoyi Hu**: Formal analysis. **Ling Zhang**: Data curation. **Nanfang Qin**: Data curation. **Huaxiang Lin**: Formal analysis. **Zhengxin Ding**: Formal analysis. **Zizhong Zhang**: Investigation, Writing – review & editing. **Jinlin Long**: Investigation, Writing – review & editing.

Declaration of Competing Interest

The authors declare that they have no known competing financial interests or personal relationships that could have appeared to influence the work reported in this paper.

Data availability

Data will be made available on request.

Acknowledgments

This work was financially supported by the National Natural Science Foundation of China (21872033 and 22102064). The Science Foundation of the Fujian Province (2022L3083). Dr. L.W. and Dr. Y.W. was supported by the Open Project Program of the State Key Laboratory of Photocatalysis on Energy and Environment (SKLPEE-KF202306), Fuzhou University.

Appendix A. Supporting information

Supplementary data associated with this article can be found in the online version at doi:10.1016/j.apcatb.2023.123636.

References

[1] T. Banerjee, F. Podjaski, J. Kröger, B.P. Biswal, B.V. Lotsch, Polymer photocatalysts for solar-to-chemical energy conversion, Nat. Rev. Mater. 6 (2021) 168–190.
[2] C. Song, Z. Wang, Z. Yin, D. Xiao, D. Ma, Principles and applications of photothermal catalysis, Chem. Catal. 2 (2022) 52–83.
[3] R. Sun, Z. Wang, Y. Li, L. Xiong, Y. Liu, Q. Wang, Design, synthesis, and insecticidal evaluation of new benzoylureas containing amide and sulfonate groups based on the sulfonylurea receptor protein binding site for diflubenzuron and glibenclamide, J. Agric. Food Chem. 61 (2013) 517–522.
[4] J. Nasser, L. Zhang, J. Lin, H. Sodano, Aramid nanofiber reinforced polymer nanocomposites via amide-amide hydrogen bonding, ACS Appl. Polym. Mater. 2 (2020) 2934–2945.
[5] I.M. Taily, D. Saha, P. Banerjee, Direct synthesis of paracetamol via site-selective electrochemical ritter-type C−H amination of phenol, Org. Lett. 24 (2022) 2310–2314.
[6] T. Yuan, Z. Wang, S. Lan, X. Gan, Design, synthesis, antiviral activity, and mechanisms of novel ferulic acid derivatives containing amide moiety, Bioorg. Chem. 128 (2022), 106054.
[7] R. Mocci, E. Colacino, L. De Luca, C. Fattuoni, A. Porcheddu, F. Delogu, The mechanochemical beckmann rearrangement: an eco-efficient “cut-and-paste” strategy to design the “Good old amide bond”, ACS Sustain. Chem. Eng. 9 (2021) 2100–2114.
[8] K. Kaur, S. Srivastava, Beckmann rearrangement catalysis: a review of recent advance, N. J. Chem. 44 (2020) 18530–18572.
[9] J.-B. Peng, H.-Q. Geng, X.-F. Wu, The chemistry of CO: carbonylation, Chem 5 (2019) 526–552.
[10] J. Han, B. Xiao, T.-Y. Sun, M. Wang, L. Jin, W. Yu, Y. Wang, D.-M. Fang, Y. Zhou, X.-F. Wu, Y.-D. Wu, J. Liao, Enantioselective double carbonylation enabled by high-valent palladium catalysis, J. Am. Chem. Soc. 144 (2022) 21800–21807.
[11] Z.-P. Bao, X.-F. Wu, Palladium-catalyzed direct carbonylation of bromoacetonitrile to synthesize 2-cyano-N-acetamide and 2-cyanoacetate compounds, Angew. Chem. Int. Ed. 62 (2023), e202301671.
[12] X. Zhang, T. Rovis, Photocatalyzed triplet sensitization of oximes using visible light provides a route to nonclassical Beckmann, Rearrange. Prod. J. Am. Chem. Soc. 143 (2021) 21211–21217.
[13] H. Lundberg, F. Tinnis, N. Selander, H. Adolfsson, Catalytic amide formation from non-activated carboxylic acids and amines, Chem. Soc. Rev. 43 (2014) 2714–2742.
[14] H. Liu, L. Zhao, Y. Yuan, Z. Xu, K. Chen, S. Qiu, H. Tan, Potassium thioacids mediated selective amide and peptide constructions enabled by visible light photoredox catalysis, ACS Catal. 6 (2016) 1732–1736.
[15] Y. Li, C. Wang, F. Zhu, Z. Wang, J.F. Soulé, P.H. Dixneuf, X.-F. Wu, An unexpected copper-catalyzed carbonylative acetylation of amines, Chem. Commun. 53 (2017) 142–144.
[16] T.N. Allah, S. Savourey, J.-C. Berthet, E. Nicolas, T. Cantat, Carbonylation of C-N bonds in tertiary amines catalyzed by low-valent iron catalysts, Angew. Chem. Int. Ed. 58 (2019) 10884–10887.
[17] R.J. Lewis, K. Ueura, X. Liu, Y. Fukuta, T.E. Davies, D.J. Morgan, L. Chen, J. Qi, J. Singleton, J.K. Edwards, S.J. Freakley, C.J. Kiely, Y. Yamamoto, G.J. Hutchings, Highly efficient catalytic production of oximes from ketones using in situ-generated H_2O_2, Science 376 (2022) 615–620.
[18] S. Kar, Q.-Q. Zhou, Y. Ben-David, D. Milstein, Catalytic furfural/5-hydroxymethyl furfural oxidation to furoic acid/furan-2,5-dicarboxylic acid with H2 production

using alkaline water as the formal oxidant, J. Am. Chem. Soc. 144 (2022) 1288–1295.
[19] Q. Wu, Y. Luo, A. Lei, J. You, Aerobic copper-promoted radical-type cleavage of coordinated cyanide anion: nitrogen transfer to aldehydes to form nitriles, J. Am. Chem. Soc. 138 (2016) 2885–2888.
[20] S. Kegnæs, J. Mielby, U.V. Mentzel, T. Jensen, P. Fristrup, A. Riisager, One-pot synthesis of amides by aerobic oxidative coupling of alcohols or aldehydes with amines using supported gold and base as catalysts, Chem. Commun. 48 (2012) 2427–2429.
[21] Y. Liang, J. Luo, D. Milstein, Facile synthesis of amides via acceptorless dehydrogenative coupling of aryl epoxides and amines, Chem. Sci. 13 (2022) 5913–5919.
[22] S. Kar, Y. Xie, Q.Q. Zhou, Y. Diskin-Posner, Y. Ben-David, D. Milstein, Near-ambient-temperature dehydrogenative synthesis of the amide bond: mechanistic insight and applications, ACS Catal. 11 (2021) 7383–7393.
[23] J. Bruffaerts, N. von Wolff, Y. Diskin-Posner, Y. Ben-David, D. Milstein, Formamides as isocyanate surrogates: a mechanistically driven approach to the development of atom-efficient, selective catalytic syntheses of ureas, carbamates, and heterocycles, J. Am. Chem. Soc. 141 (2019) 16486–16493.
[24] R.A. Singer, S. Monfette, D. Bernhardson, S. Tcyrulnikov, A.K. Hubbell, E. C. Hansen, Recent advances in nonprecious metal catalysis, Org. Process Res. Dev. 25 (2021) 1802–1815.
[25] C. Chen, J.C. Peters, G.C. Fu, Photoinduced copper-catalysed asymmetric amidation via ligand cooperativity, Nature 596 (2021) 250–256.
[26] J.-X. Hu, L. Luo, X.-J. Lv, L. Liu, Q. Liu, Y.-K. Yang, C.-Y. Duan, Y. Luo, T. Liu, Light-induced bidirectional metal-to-metal charge transfer in a linear Fe_2Co cluster, Angew. Chem. Int. Ed. 56 (2017) 7663–7668.
[27] D. Wei, C. Darcel, Iron catalysis in reduction and hydrometalation reactions, Chem. Rev. 119 (2019) 2550–2610.
[28] H. Zou, S. Zhu, Progresses of 1,10-phenanthroline type ligands in Fe/Co/Ni Catalysis, Prog. Chem. 32 (2020) 1766–1803.
[29] E. Vahidzadeh, S. Zeng, K.M. Alam, P. Kumar, S. Riddell, N. Chaulagain, S. Gusarov, A.E. Kobryn, K. Shankar, Harvesting hot holes in plasmon-coupled ultrathin photoanodes for high-performance photoelectrochemical water splitting, ACS Appl. Mater. Inter. 13 (2021) 42741–42752.
[30] X. Meng, L. Liu, S. Ouyang, H. Xu, D. Wang, N. Zhao, J. Ye, Nanometals for solar-to-chemical energy conversion: from semiconductor-based photocatalysis to plasmon-mediated photocatalysis and photo-thermocatalysis, Adv. Mater. 28 (2016) 6781–6803.
[31] Y. Qi, J. Jiang, X. Liang, S. Ouyang, W. Mi, S. Ning, L. Zhao, J. Ye, Fabrication of black In_2O_3 with dense oxygen vacancy through dual functional carbon doping for enhancing photothermal CO_2 hydrogenation, Adv. Funct. Mater. 31 (2021) 2100908.
[32] S.-G. Xia, Z. Zhang, J.-N. Wu, Y. Wang, M.-J. Sun, Y. Cui, C.-L. Zhao, J.-Y. Zhong, W. Cao, H. Wang, M. Zhang, Y.-C. Zheng, X.-B. Li, Cobalt carbide nanosheets as effective catalysts toward photothermal degradation of mustard-gas simulants under solar light, Appl. Catal. B Environ. 284 (2021), 119703.
[33] Z. Wu, C. Li, Z. Li, K. Feng, M. Cai, D. Zhang, S. Wang, M. Chu, C. Zhang, J. Shen, Z. Huang, Y. Xiao, G.A. Ozin, X. Zhang, L. He, Niobium and titanium carbides (MXenes) as superior photothermal supports for CO_2 photocatalysis, ACS Nano 15 (2021) 5696–5705.
[34] L. Wang, R. Sa, Y. Wei, X. Ma, C. Lu, H. Huang, E. Fron, M. Liu, W. Wang, S. Huang, J. Hofkens, M.B.J. Roeffaers, Y. Wang, J. Wang, J. Long, X. Fu, R. Yuan, Near-infrared light-driven photoredox catalysis by transition-metal-complex nanodots, Angew. Chem. Int. Ed. 61 (2022), e202204561.
[35] W.-T. Huang, T.-Y. Su, M.-H. Chan, J.-Y. Tsai, Y.-Y. Do, P.-L. Huang, M. Hsiao, R.-S. Liu, Near-infrared nanophosphor embedded in mesoporous silica nanoparticle with high light-harvesting efficiency for dual photosystem enhancement, Angew. Chem. Int. Ed. 60 (2021) 6955–6959.
[36] A. Jeantet, Y. Chassagneux, T. Claude, P. Roussignol, J.S. Lauret, J. Reichel, C. Voisin, Exploiting one-dimensional exciton-phonon coupling for tunable and efficient single-photon generation with a carbon nanotube, Nano Lett. 17 (2017) 4184–4188.
[37] S. Guddala, F. Komissarenko, S. Kiriushechkina, A. Vakulenko, M. Li, V.M. Menon, A. Alù, A.B. Khanikaev, Topological phonon-polariton funneling in midinfrared metasurfaces, Science 374 (2021) 225–227.
[38] Y. Guo, L. Mao, Y. Tang, Q. Shang, X. Cai, J. Zhang, H. Hu, X. Tan, L. Liu, H. Wang, T. Yu, J. Ye, Concentrating electron and activating H-OH bond of absorbed water on metallic $NiCo_2S_4$ boosting photocatalytic hydrogen evolution, Nano Energy 95 (2022), 107028.
[39] S. Jiang, C. Li, Y. Mahammad, Y. Tang, R. Wang, J. Li, J. Li, Z. Zhao, Z. Zhao, Solvent-induced fabrication of Cu/MnOx nanosheets with abundant oxygen vacancies for efficient and long-lasting photothermal catalytic degradation of humid toluene vapor, Appl. Catal. B Environ. 328 (2023), 122509.
[40] F. Feng, H. Guo, D. Li, C. Wu, J. Wu, W. Zhang, S. Fan, Y. Yang, X. Wu, J. Yang, B. Ye, Y. Xie, Highly efficient photothermal effect by atomic-thickness confinement in two-dimensional ZrNCl nanosheets, ACS Nano 9 (2015) 1683–1691.
[41] L. Lin, E.H. Hill, X. Peng, Y. Zheng, Optothermal manipulations of colloidal particles and living cells, Acc. Chem. Res. 51 (2018) 1465–1474.
[42] X. Cui, Q. Ruan, X. Zhuo, X. Xia, J. Hu, R. Fu, Y. Li, J. Wang, H. Xu, Photothermal nanomaterials: a powerful light-to-heat converter, Chem. Rev. 123 (2023) 6891–6952.
[43] K. Ratzenböck, M.M.U. Din, S.M. Fischer, E. Žagar, D. Pahovnik, A.D. Boese, D. Rettenwander, C. Slugovc, Water as a monomer: synthesis of an aliphatic polyethersulfone from divinyl sulfone and water, Chem. Sci. 13 (2022) 6920–6928.
[44] Q. Liu, J. Yuan, Z. Gan, C. Liu, J. Li, Y. Liang, R. Chen, Photocatalytic N_2 reduction: uncertainties in the determination of ammonia production, ACS Sustain. Chem. Eng. 9 (2021) 560–568.